Design, Synthesis and Biological Evaluation of Chalcone Acetamide Derivatives against Triple Negative Breast Cancer

Puneet Kumar[1,4], Ruhi Singh[2], Deepak Sharma[1], Qazi Parvaiz Hassan[3], Boobalan Gopu[2,4], Jasha Momo H. Anal[1,4,*]

[1]Natural Products and Medicinal Chemistry Division, CSIR– Indian Institute of Integrative Medicine, Jammu-180001, India

[2]Pharmacology Division, CSIR– Indian Institute of Integrative Medicine, Jammu-180001, India

[3]Biotechnology Division, CSIR – Indian Institute of Integrative Medicine, Sanatnagar, Srinagar – 190005, India

[4]Academy of Scientific and Innovative Research (AcSIR), Ghaziabad – 201002, India

Puneet Kumar and Ruhi Singh contributed equally to this study.

[*]Correspondence:

Jasha Momo H. Anal, Natural Products and Medicinal Chemistry Division, CSIR– Indian Institute of Integrative Medicine, Jammu-180001, India. Email: hmunshel.jasha@iiim.res.in

Abstract

Breast Cancer (BC) incidence rates increased (0.5%) annually in recent decades with moderate mortality. Triple-negative breast cancer (TNBC) poses molecularly diversified tumor aggressiveness, heterogeneous illness, recurrence, and high risk of metastasis. TNBC patients have poor prognosis due to later-stage diagnosis and fewer treatment options than other subtypes. Chalcones are chemical scaffolds found in natural products, especially in plants, considered diverse and structurally privileged in medicinal chemistry for drug development. Herein, we designed and synthesized novel acetamide derivatives of chalcone to evaluate against TNBC, and characterized them using ^{1}H NMR, ^{13}C NMR, HRMS and IR spectroscopic methods. The derivatives were screened against human cancer cells for their cytotoxicity using SRB assay. Among the derivatives, **8h** with the pyrrolidine group exhibited better cell growth inhibitor activity against both TNBC (MDA-MB-231 and MDA-MB-468) cells. SRB, Colony formation and fluorescent dye-based screening assays demonstrated that **8h** significantly inhibited MDA-MB-231 cell proliferation. Furthermore, **8h** promoted apoptosis *via* upregulation of the cellular reactive oxygen species (ROS) levels and loss of mitochondrial membrane potential. **8h** increased the pro-apoptotic proteins (Bax and caspase-3) and Bax/Bcl-2 ratio, inhibiting the anti-apoptotic (Bcl-2) protein levels in TNBC cells. The above results suggest that **8h** can promote cellular death through apoptotic mechanisms in TNBC cells, and this hypothesis confirms that chalcones can be designed with potential cytotoxicity against TNBC.

Keywords: Chalcone; triple-negative breast cancer; Acetamide derivatives; Apoptosis; MDA-MB-231

1. INTRODUCTION

Breast cancer is the most diagnosed cancer, and its malignancy in women impairs the country's healthcare system (Siegel et al. 2022). Its incidence rates are growing in transitioning countries, contributing to 25% of all female cancer cases (Heer et al. 2020). Triple-negative breast cancer (TNBC) is a heterogeneous disease involving distant metastasis to the brain and visceral organs. Metastatic TNBC (mTNBC) patients have poorer 5-year overall survival rates (10.81%) than their metastatic non-TNBC (33.46%) molecular types. The absence of specific target receptors like the estrogen receptor (ER), progesterone receptor (PR), and human epidermal growth factor receptor 2 (HER2) limited the therapeutic approaches to treat TNBC (Pareja et al. 2016). TNBC lacks targeted proteins, resulting in untargeted therapy, poor patient outcomes, higher tumor-initiating and self-renewal potential and promoting therapy resistance, proliferation and high recurrence (Hsu et al. 2022). Taxane-based first-line chemotherapy significantly improves the patient's quality of life and overall survival, but its application is limited due to chemo-resistance activity and toxicity. The FDA approved the PARP inhibitors (Olaparib) and immunotherapeutic (Pembrolizumab) agents to be used in combination with chemotherapy agents to treat TNBC (Pareja et al. 2016; Schmid et al. 2020). Therefore, developing novel TNBC mono-chemotherapeutic agents with lower toxicity is an urgent medical need.

Chalcones are privileged structures and scaffolds in medicinal chemistry for drug discovery (Marotta et al. 2022; Zhuang et al. 2017). Chalcones are abundant in plant sources and are key intermediate metabolites of the flavonoid biosynthetic pathway in plants. Chalcones contain two aromatic rings in their structure linked with α, ß-unsaturated ketone moiety, exhibit structural heterogeneity and provide a broad spectrum of pharmacological activities, including anticancer properties (Das and Manna 2016; Ouyang et al. 2021). Chalcones derivatives isolated from diverse natural sources known for cytotoxic activities on various cancer cells (Blanquer-Rossello et al. 2013; Gao et al. 2021; Huang et al. 2020; Simirgiotis et al. 2008; Venturelli et al. 2016; Zhang et al. 2022). Clinical approval of chalcone-based (metochalcone, sofalcone and hesperidin methylchalcone) drugs also emphasizes the chalcone moiety as a potential template for developing novel anticancer agents (Fig. 1). Chalcone's small structures and Michael's acceptor properties attract medicinal chemist approaches to design their derivatives and structural activity relationships (SAR) for increased activities (Das and Manna 2016; Gomes et al. 2017b; Liu et al. 2003; Sahu et al. 2012). Also, the reports affirm that minor structural modification of chalcones with functional group addition enables chalcone binding with varied targets and significantly affects their pharmacological activities, *viz*., druggability, potency and dose (Gomes et al. 2017a).

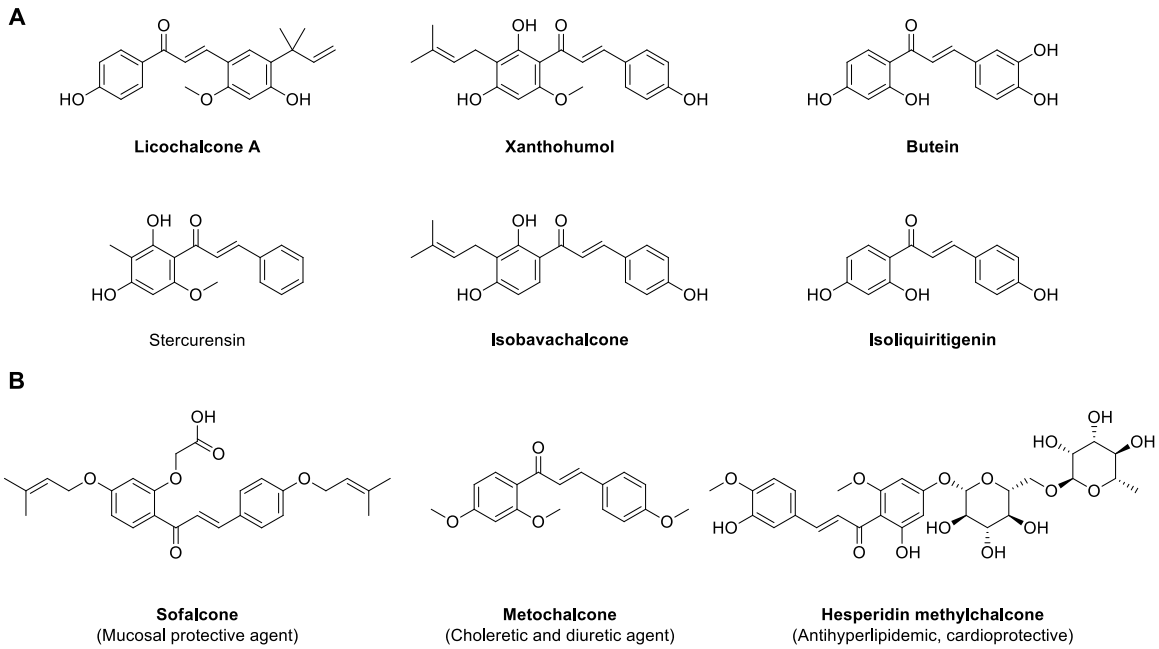

Fig. 1. Chalcone compounds with pharmacological activities. A: Naturally occurring chalcones with anti-proliferative activity. B: Clinically approved Chalcone-based drugs.

To develop novel anticancer agents, we chemically synthesized a series of acetamide derivatives of chalcone (**8a-8l**) by structural modification. We screened its anticancer activities against a panel of human cancer cell lines in vitro using SRB assay. Further, the apoptotic potential and nuclear morphological changeability of potent compound **8h** were assessed by fluorescent-dye-based methods (DAPI, ROS and MMP). Western blotting techniques are also performed to confirm the increased apoptotic protein expression.

2. MATERIALS AND METHODS

2.1. Experimental procedure for the synthesis of chalcone

In a round bottom flask, 4-hydroxy acetophenone (1 eq.) and 4-methoxy benzaldehyde (1 eq.) were taken, dissolved in ethanol and aqueous 10% NaOH was introduced dropwise. This mixture was kept on stirring at room temperature for 6 hrs. The reaction was observed in the TLC plate using the 20% ethyl acetate:hexane mobile phase. After completion of the reaction, cold water (5 ml) was added, and 1N HCl was used to precipitate the product into a yellowish precipitate. The residue was crystallized with methanol to get the pure compound, as shown in Scheme 1 (Rahimzadeh Oskuei et al. 2021; Yamali et al. 2017).

2.2. Synthesis of the Chalcone amide derivatives

Primary or secondary amines (1 eq.) were added in DCM with triethylamine (1.2 eq.) in a round bottom flask, and chloroacetyl chloride (1.1 eq.) was added dropwise to the mixture at 0°C. The resulting mixture was stirred for 3 hrs at room temperature. After observing the reaction in TLC, the solvent was evaporated on rotavapour, and then a work-up was done with organic solvent (ethylacetate) and water. The ethyl acetate layer was collected and dried with Na_2SO_4, and the solvent was evaporated using rotavapour; this gives us chloroacetamide derivatives **(7a-7l)**, used without purification. The procedure was followed with slight modifications from the published reports, as shown in Scheme 2 (Trapero et al. 2018).

Further, chalcone (1 eq.) **(4)** and chloroacetamide (1 eq.) **(7a-7l)** derivatives were added in the round bottom flask, and dimethyl formamide (DMF) and K_2CO_3 (3 eq.) were added. At room temperature, the reaction lasted for 6 hrs. The reaction was monitored in TLC, and a work-up was done with ethyl acetate and water. The ethyl acetate layer was collected and dried over rotavapour to get the final crude product and purified from column chromatography using 30% ethyl acetate: hexane solvent as a mobile phase to give the final product **(8a-8l)** as shown in Scheme 3 and Fig.2.

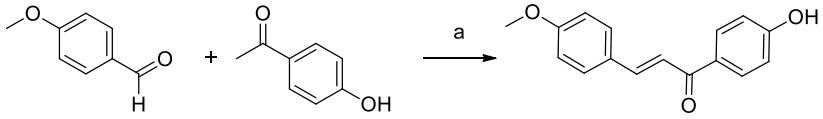

2 **3** **4**

Scheme 1

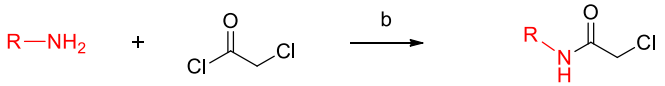

5 **6** **7(a-l)**

Scheme 2

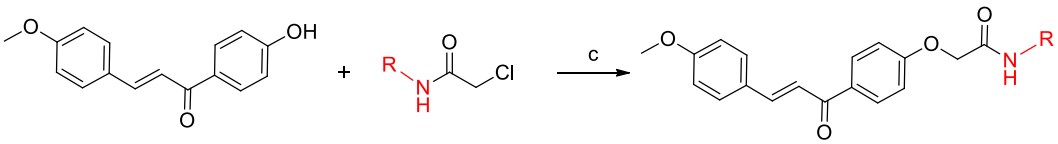

4 **7(a-l)** **8(a-l)**

Scheme 3

Schemes: Synthesis of different acetamide derivatives of chalcone (**8a-8l**) using a Claisen-Schmidt reaction. (a): 10% NaOH, EtOH, RT, 6 hrs, yield - 90%; (b): Et_3N, DCM, 0°C-RT, 3 hrs, yield - 80-85%; (c) K_2CO_3, DMF, RT, 6 hrs, yield, 75-85%.

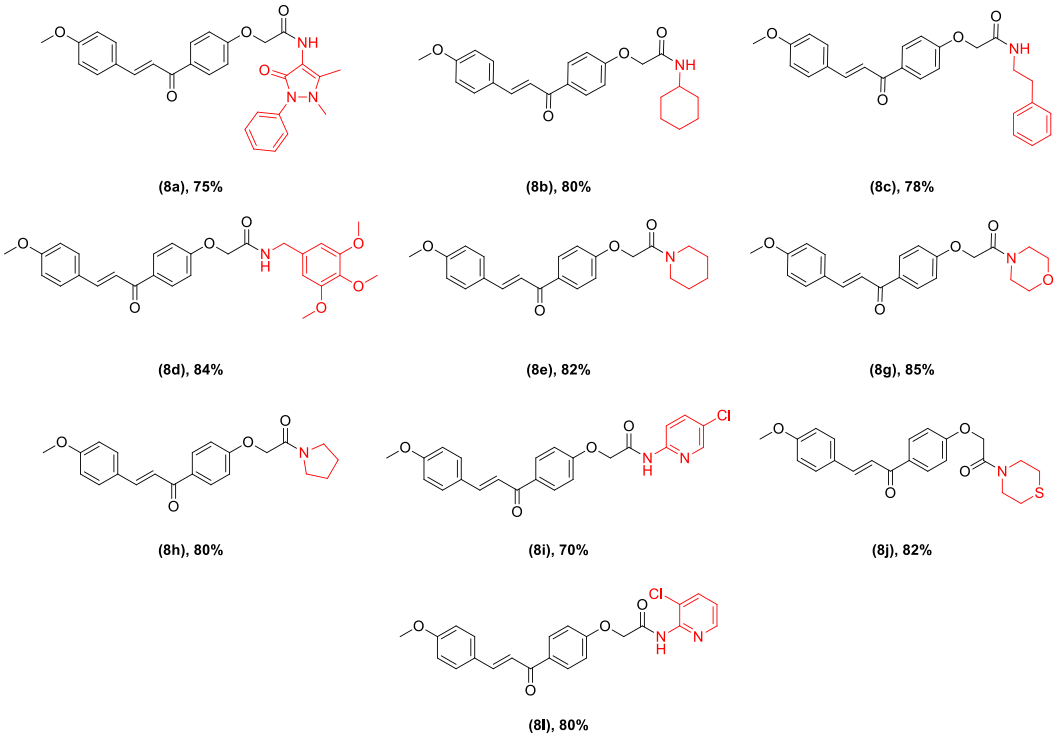

Fig. 1. Chemical structure of synthesized chalcone acetamide derivatives

2.3. Cell cultures

A panel of human cancer cell lines procured from American Type Culture Collection (ATCC) was used for the study, which includes Breast (MDA-MB-231, MDA-MB-468 and MCF-7), Lung (A549), and Colon (HCT116), and normal human embryonic kidney epithelial cell (HEK-293). Cells were cultured in RPMI/DMEM (Thermo-Gibco) media supplemented with 10% FBS (Thermo-Gibco), Penicillin (100U/ml) and Streptomycin (100µg/ml) (Thermo-Gibco) for the growth of the cells. All cell lines were then maintained in a CO_2 incubator at 37ºC with 95% humidity and 5% CO_2.

2.4. Sulforhodamine B assay

Using Sulforhodamine B (SRB, Sigma-Aldrich) dye, pH-dependent staining of proteins assay was performed on the treated plates to evaluate the anticancer potential of the novel compounds. Briefly, cells were seeded in 96-well flat bottom plates at the required density based on the cell lines, and their morphology was observed under a bright field microscope. After 24 hrs of CO_2 incubation, cells were treated with chalcone derivatives in triplets. Paclitaxel (Sigma-Aldrich) was used as the positive control as it has been reported to have anticancer potential against several cancer cell lines. The plates were then incubated for 48 hrs under the above-prescribed conditions.

The cells were fixed using 50% (w/v) trichloro acetic acid (TCA) (Sigma-Aldrich) at 4ºC for 1 hrs. Plates were then washed with water and kept overnight for drying. Then, plates were stained with 100µl of SRB dye (0.4% w/v in 1% acetic acid) (Sigma-Aldrich) at room temperature for 1 hrs. The plates were washed with 1% (v/v) glacial acetic acid (SRL Chemicals) to remove the unbound SRB dye and were kept overnight for air drying. 100µl of 10mM Tris base (Sigma-Aldrich) solution was added to each well for the plate to solubilize the protein-bound SRB, shaken for 10 minutes, and the optical density was measured at the wavelength of 540 nm using a multimode microplate reader (TecanTM Infinite® M-Plex). The cell growth inhibition (%) and IC50 (lowest dose causing 50% cancer cell growth inhibition) were calculated using non-linear regression analysis in GraphPadTM PRISM 7.0 software. IC_{50} was used to indicate the cytotoxic effect of the synthesized compounds with reference to untreated control cells.

2.5. Clonogenic assay

The clonogenic cell survival assay assesses a cell's capacity to divide while maintaining its capacity to give rise to a large colony or a clone. The reproductive integrity of MDA-MB-231 cells against the concentration of **8h** was evaluated. Cells were cultured in 6-well plates at a density of 1×10^4 cells per ml/well and treated for **8h** with four different concentrations for 24 hrs. Following the treatment, the medium was changed on alternate days for 7 days. The resulting colonies were stained with 0.5% crystal violet (Sigma-Aldrich) solution and preserved with 4% paraformaldehyde (Sigma-Aldrich). After 30 minutes, the liquid mixture was removed, and the plates were rinsed with PBS (Thermo-Gibco) and left to air dry. Randomly selected colonies from the observed fields were counted, averaged, and captured using a mobile phone camera (iPhone 13 mini). The magnified image of the control and **8h** (8µM) was captured using a microscope (Olympus IX53).

2.6. DAPI Assay

DAPI dye (Sigma-Aldrich) was used to stain the nucleus to assess apoptosis determined by nuclear damage**.** MDA-MB-231 cells were seeded @ 1×10^5 cells per well of a 6-well plate and were kept in an incubator overnight (37ºC and 5% CO_2) for the cells to attain their morphology for 24 hrs. The cells were treated with four different (4µM, 8µM, 12µM and 16µM) concentrations of **8h** for 48 hrs. The cells were given PBS (Thermo-Gibco) wash twice and were fixed in ice-cold 4% paraformaldehyde (Sigma-Aldrich). Further, cells were permeabilized with 0.35% Triton-X-100 (Sigma-Aldrich) and stained with DAPI dye. The cells were washed with PBS after 30 minutes of incubation and were observed for fluorescence intensity under the fluorescent microscope (Olympus IX53).

2.7. Generation of Reactive Oxygen Species (ROS)

An increase in the generation of ROS is the primary indication of apoptosis in a cell. 1×10^5 MDA-MB-231 cells per well were seeded on a 6-well plate and were incubated for 24 hrs in a humidified incubator for cell adherence and to attain their morphology. Cells were then treated with different concentrations of **8h** for 48 hrs. After 48 hrs of treatment, 10µm of DCFDA dye (Sigma-Aldrich) was added to each well and cells were incubated for 30 minutes. H_2O_2 (0.05%) was added as a positive control, which is known to elicit intracellular ROS generation. All the wells were washed with PBS (Thermo-Gibco), and fluorescence images were captured using a fluorescence microscope.

2.8. Mitochondrial Membrane Potential Assay

Loss of mitochondrial membrane potential (MMP) is caused by the cytoplasmic release of apoptogenic stimuli, disrupting mitochondrial membrane potential and cell death**.** Rhodamine-123 enters active mitochondria due to its negative MMP. MDA-MB-231 cells seeded @ 1×10^5 cells per well of a 6-well plate incubated under the above-prescribed conditions for 24 hrs. Cells were then treated with **8h** at different concentrations for 48 hrs. Cells were given PBS (Thermo-Gibco) wash twice, 1ml of 200 nm of Rhodamine-123 dye (Sigma-Aldrich) was added to each well, and the plate was incubated for 15 minutes to allow the cells to take up the dye. After 15 minutes, wells were washed with PBS thrice, and a final volume (1ml) of incomplete media was added to each well to visualize the cells under a fluorescent microscope.

2.9. Western Blot analysis

Briefly, MDA-MB-231 cells were lysed on ice at a concentration of 3×10^6 cells for 2 minutes with RIPA lysis buffer (0.5 mM sodium orthovandate, 2 mM phenylmethylsulfonyl fluoride, 50 mM sodium fluoride, and protease inhibitor). The treated cells were centrifuged at 12000 g for 20 minutes, and supernatant from each sample was then combined with an equivalent volume of 2X gel-loading sample buffer. SDS-PAGE analysis of the protein lysates and common protein markers was performed. On SDS PAGE, protein aliquots (70 µg) were resolved and were electro-transferred to Polyvinylidene Fluoride (PVDF) membranes at 4˚C for 2 hrs in an ice-cold transfer buffer. Non-specific membrane bindings were blocked with 5% Bovine Serum Albumin for 1 hr at room temperature and were prevented and then incubated with antibodies against Bax, Bcl-2 and caspase-3 purchased from CST (Danvers, Massachusetts, USA) overnight. Blots washed with TBST three times and treated with corresponding HRP-conjugate secondary antibodies for 1hr (1:1000 dilution). β-actin is used as the housekeeping protein. Protein expression after treatment with substrate luminol was detected by chemiluminescence using the ChemiDoc Imaging System (Bio-Rad, California, USA).

2.10. Statistical Analysis

All data were analyzed and plotted using GraphPad™ Prism (Ver. 7.0), Image J (ver. 1.54) and Tableau® licensed version (Ver. 2023.2.0) software. Significant difference of the groups in comparison to control were analyzed using appropriate methods mentioned in each image captions.

3. RESULTS AND DISCUSSIONS

3.1. Chemistry

We have designed and synthesized the acetamide derivatives of chalcone to study their anticancer activity. Compound **4** was synthesized using 4-hydroxyacetophenone (**2**) and 4-methoxy benzaldehyde (**3**) by Claisen–Schmidt reaction using previously reported method (Rahimzadeh Oskuei et al. 2021; Yamali et al. 2017), shown in Scheme 1. Treatment of primary and secondary amine derivatives (**5**) with chloroacetyl chloride (**6**) in the presence of TEA afford chloroacetamide (**7a-7l**). This chloroacetamide was further substituted at the hydroxy group present in aromatic ring A of chalcone **(4)** in the presence of K_2CO_3 and DMF to form chalcone acetamide derivatives (**8a-8l**). Different spectroscopic techniques (HRMS, ^{1}H and ^{13}C NMR spectroscopy) were used to characterize newly synthesized compounds.

The coupling constant (*J*) values of 15–16 Hz indicate that the chalcone moiety's double bond is in the trans-configuration. In the ^{13}C NMR spectrum, the characteristic peak of carbonyl carbon in chalcone moiety was observed in the range of δ 180-190 and the peak of carbonyl carbon of amide bond appeared in the range δ 164-169 olefinic bond carbon, and aromatic carbon comes in the range of δ 163–104. The HRMS (ESI) of all the compounds showed an $[M+H]^+$ peak equivalent to their molecular formulae.

3.2. SRB assay

All acetamide derivatives of chalcone were investigated using SRB assay against a panel of cancer cell lines, including TNBC (MDA-MB-231 and MDA-MB-468), Non-TNBC (MCF-7), Colon (HCT116) and Lung (A549) cells and paclitaxel was taken as reference control. All derivatives were assessed for toxicity on healthy non-cancerous kidney cells (HEK293) to confirm their selectivity towards cancerous cells. The *in vitro* cell viability (%) results are summarized in Fig. 3

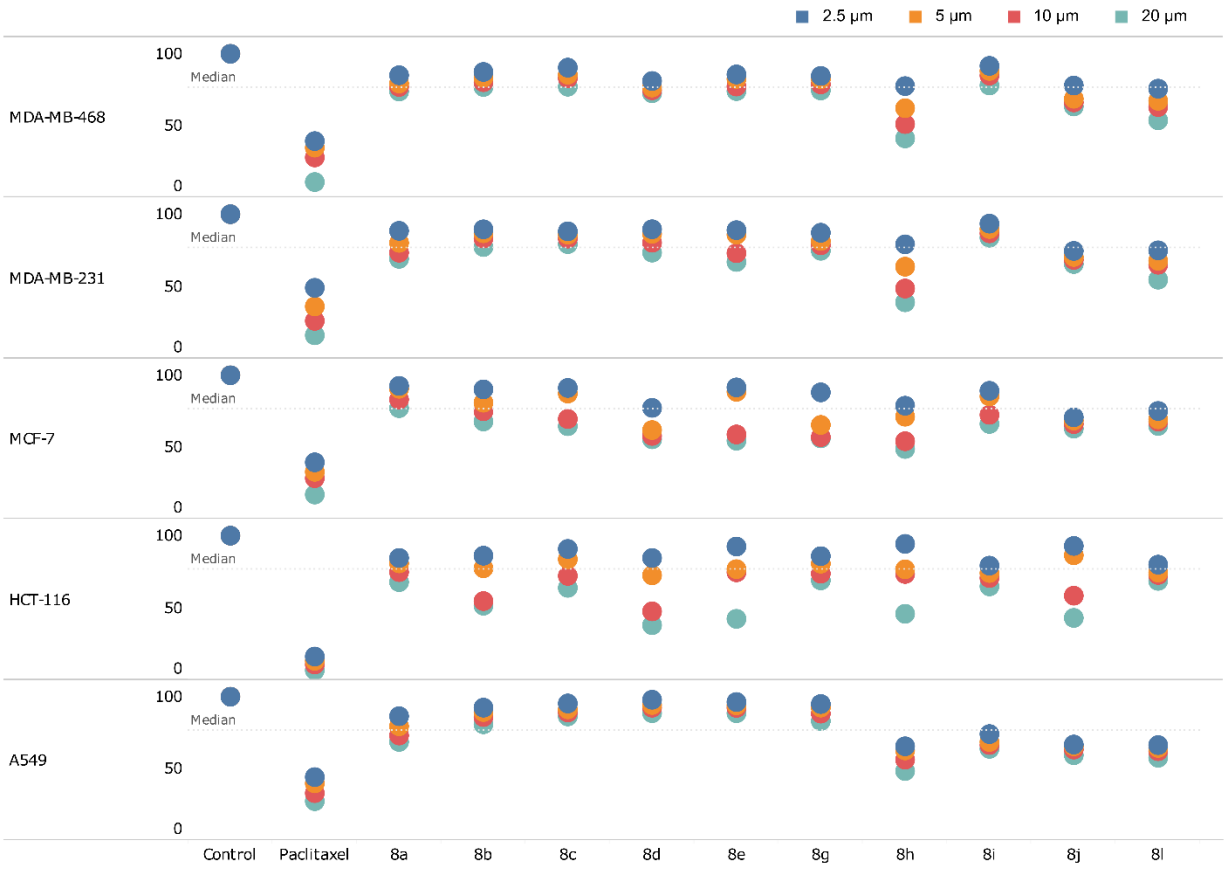

Fig. 3: Comparison of acetamide derivatives cell viability (%) against all cell lines at four different concentrations. The graph was plotted using the Tableau® software licensed version (Ver. 2023.2.0).

A broad spectrum of lethality was observed on all compounds against these cancer cell lines and promising activities on HCT116 with varying growth inhibition (Fig.3). Compounds **8b**, **8d**, **8e**, and **8j**, containing different heterocyclic and aromatic rings, exhibited comparable inhibition with IC_{50} values ranging from 10.53-18.95 µM against HCT116 cells after 48 hrs of the treatment (Table 1). Derivative **8e** containing a six-membered piperidine ring showed efficacy only in ER+ breast cancer (MCF-7) and Colon (HCT116) cells. Similarly, **8j**, which contains thiomorpholine moiety, displayed 3-fold more activities against HCT116 (IC_{50} – 15.19±0.50 µM) than A549 cells (IC_{50} - 45.35±2.09 µM). **8l** showed similar efficacy against TNBC and lung cancer cell lines with IC_{50} more than 24 µM.

Table 1: IC_{50} of synthesized chalcones using SRB assay

Compounds	IC_{50} [a,b](μM)				
	MDA-MB-231	**MDA-MB-468**	**MCF-7**	**HCT116**	**A549**
8a	ND[c]	ND	ND	ND	ND
8b	ND	ND	ND	18.95±0.48	ND
8c	ND	ND	ND	ND	ND
8d	ND	ND	ND	10.53±0.03	ND
8e	ND	ND	22.70±1.68	17.36±0.23	ND
8g	ND	ND	ND	ND	ND
8h	**9.42±0.45**	**10.13±0.29**	16.20±0.40	18.30±0.43	17.12±0.85
8i	ND	ND	ND	ND	ND
8j	ND	ND	ND	15.19±0.50	45.35±2.09
8l	24.12±0.16	25.25±0.02	ND	ND	35.40±3.23

[a]Each compound was tested for cytotoxicity in triplicate. IC_{50} data are expressed as mean±SEM (n=3).
[b]The concentrations exhibiting 50% cell growth inhibition (IC_{50}) after 48h of the treatment were determined using GraphPad™ Prism 7.0 Software.
[c]Not detected

However, only **8h** containing pyrrolidine ring shows potential cell viability (%) reduction of all cancer cells among all the derivatives. Also, the inhibition rates increased with the concentration levels of **8h**, providing its best cytotoxicity at 20 μM concentration in these cells (Fig. 3 and 4). Furthermore, **8h** showed relatively low toxic effects on both colon (HCT116) and Lung (A549) cancer cells at all concentrations compared to breast cancer cells. Incidentally, high growth (~60%) inhibition activity of **8h** was observed at 20 μM concentration against TNBC cell lines (Fig. 4).

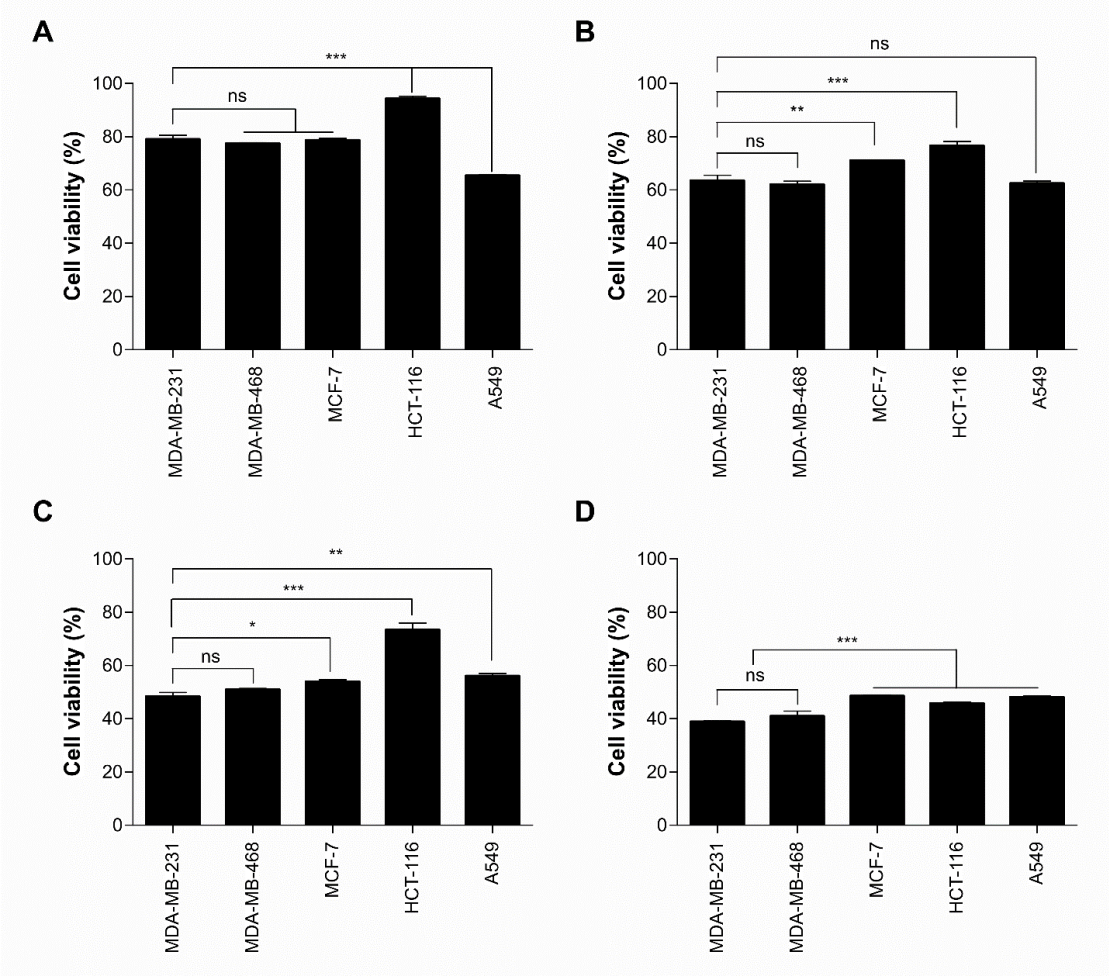

Fig. 4: Comparison of cell viability (%) of **8h** at different concentrations. **8h** were tested for cell viability in triplicate at four different concentrations (A: 2.5 µM, B: 5 µM, C: 10 µM, D: 20 µM) using human cancer cell lines. Cell viability graphs are expressed as mean±SEM (n=3) and plotted using GraphPad™ Prism 7.0 Software. MDA-MB-231 cells were compared against other cancer cells for significance by applying One-way ANOVA with Dunnet's multiple comparison test. ^{ns} non-significant * $P < 0.05$, ** $P < 0.01$, *** $P < 0.001$.

Compound **8h** activity against TNBC cells (MDA-MB-231 and MDA-MB-468) are comparable in efficacy related to *in vitro* cytotoxicity and IC_{50} values and significance observed over non-TNBC (MCF-7) cells at all concentrations (Table 1 and 2; Fig. 4 and 5A). Most importantly, **8h** exhibited the most potent cytotoxicity with single-digit IC_{50} (9.42±0.45 µM) value against MDA-MB-231 cells compared to MDA-MB-468 (IC_{50} – 10.13±0.29µM) and MCF-7 (IC_{50} – 16.20±0.40µM) cells (Table 2; Fig. 3A). From the findings of *in vitro* cytotoxicity, it was noticeable that the amide bond formed with the nitrogen of five-membered heterocyclic ring (secondary amine) attached to chalcone in ring A, resulting in a significant increase in potency

when compared with the amide bond formed with the amine group (primary amine). Interestingly, when normal HEK293 cells were incubated with **8h**, there was more than 4-fold less cytotoxicity in HEK293 than in MDA-MD-231 cells (Table 2; Fig. 5B). Since MDA-MB-231 is a cell line model for a more aggressive, hormone-independent breast cancer with fewer treatment options and compound **8h** had a higher selectivity index, validating its least toxic nature, allowing further proceedings for mechanistic studies to determine its mechanism of action.

Table 1: IC_{50} and selectivity index (SI) of **8h**

Cell Line	IC_{50} [a,b](μM)	Selectivity Index (SI) wrt to HEK[c] cell line
MDA-MB-231	9.42±0.45	4.14±0.13
MDA-MB-468	10.13±0.29	3.87±0.33
MCF-7	16.20±0.40	2.42±0.22

[a]8h were tested for cell viability (%) against breast cancer cells in triplicate at four different concentrations
[b]50% inhibitory concentration (IC50) after 48 hrs of the treatment was determined using GraphPad™ Prism 7.0 Software; IC_{50} and SI data are expressed as mean±SEM, n=3.
[c]human embryonic kidney cells

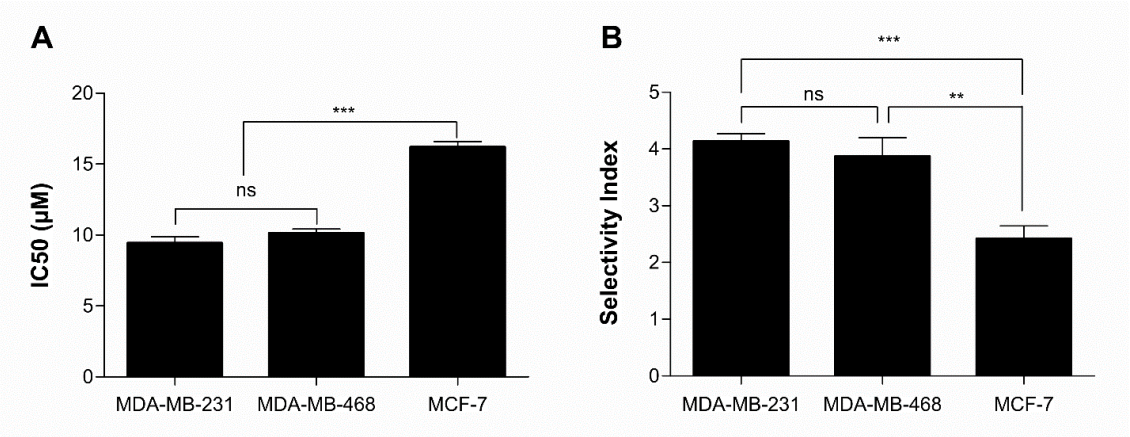

Fig. 5: Bar graph represents IC_{50} and Selectivity Index (SI) of **8h** against a human breast carcinoma cell line panel. Graphs are expressed as mean±SEM (n=3) and plotted using GraphPad™ Prism 7.0 Software. MDA-MB-231 cells were compared against other breast cancer cells for significance by applying One-way ANOVA with Dunnet's multiple comparison test. [ns] non-significant * $P < 0.05$, ** $P < 0.01$, *** $P < 0.001$.

3.3. Colony growth inhibition

The antiproliferative potential of **8h** and its ability to control the growth of pre-formed colonies is evaluated using a clonogenic assay. From the figure representation in the untreated group, overlapping colonies of MDA-MB-231 cells were observed (Fig. 6B). MDA-MB-231 cells colonies were significantly attenuated by **8h** treatment in a concentration-dependent manner, and

only a fraction of seeded cells retained the capacity to produce colonies. **8h** treatment significantly ($p<0.001$) reduced both the size and the number of colonies in MDA-MB-231 cells in comparison to untreated cells and thereby suppressed the colony-forming ability of MDA-MB-231 cells (Fig. 6A and 6C).

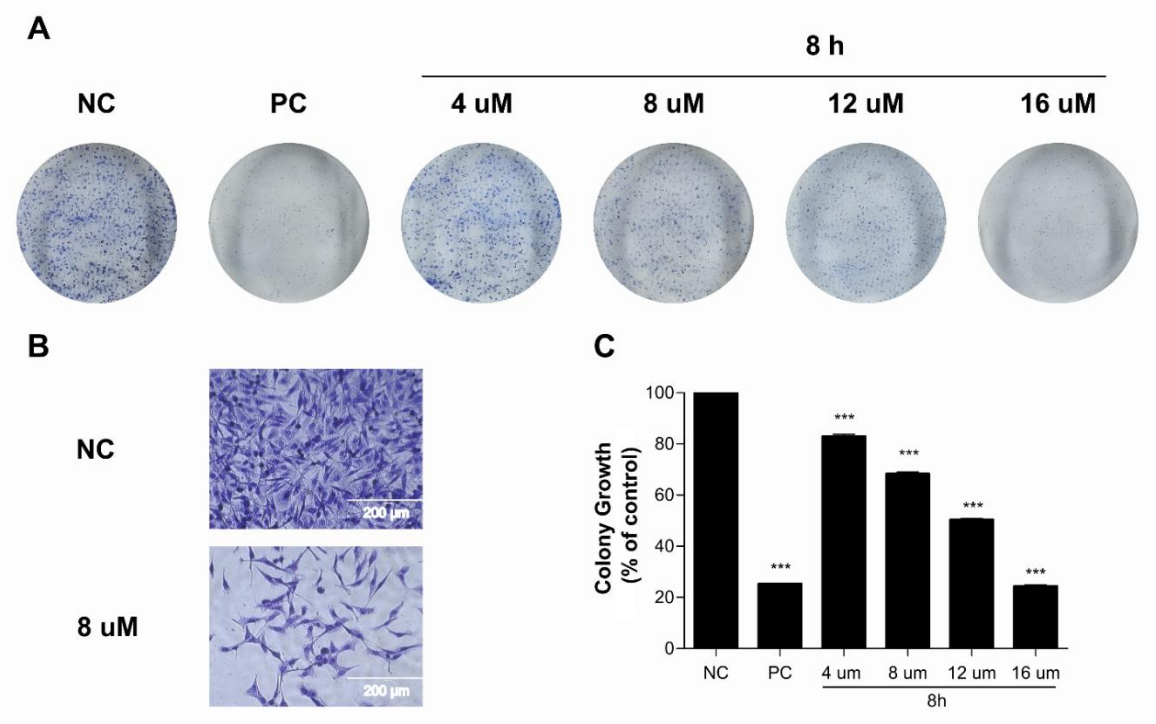

Fig. 6: 8h inhibits colony formation in MDA-MB-231 cells. A-B: Representative images of colony growth inhibition of MDA-MB-231 cells treated with an indicated concentration of **8h** for 24h. Paclitaxel (0.5 µM) was used as a Positive control. A: No magnification, B: Scale bar 200 µm. C: Colonies were quantified using Image J software (ver. 1.54) and plotted as mean±SEM (n=3) graphs using GraphPad™ Prism 7.0 Software. Statistical significance was compared with untreated control by applying One-way ANOVA with Dunnet's multiple comparison test. *** $P < 0.001$.

3.4. Apoptosis induction evaluation

Comprehensive literature indicated that chalcone derivatives induce apoptosis in various cancer cells (Kamal et al. 2010; Khusnutdinova et al. 2021; Steinlein et al. 2023; Wang et al. 2022; Zhao et al. 2017). The untreated cells in negative control were present in large quantities compared to treated cells observed using a fluorescent microscope and DAPI assay (Fig. 7A). Cellular nuclear morphology in untreated cells is well-defined and homogenously stained, whereas the cells treated with positive control and different concentrations of **8h** show apoptotic effect along with the chromatin condensation and blebbing, which are hallmarks of apoptosis

Similarly, ROS are highly reactive molecules that are essential to regulate the apoptosis of cells. A rise in ROS levels alters cancer cells' microenvironments and metabolic pathways, which may result in oxidative stress and cell apoptosis (Kim et al. 2016; Trachootham et al. 2009). MDA-MB-231 cells were treated with different concentrations of **8h** for 48 hrs, stained with DCFDA and observed under the fluorescent microscope. **8h** significantly induced ROS generation in MDA-MB-231 cells in a dose-dependent manner compared to the untreated control group (Fig. 7B and 7D). Similar results of H_2O_2 as a positive control were observed.

Further, in the apoptotic cascade, mitochondrial membrane potential (MMP) alterations are essential and are detected using Rhodamine-123 dye (Gottlieb et al. 2003). Generally, fluorescence intensity decreases when early apoptosis occurs with loss of mitochondrial integrity and MMP. MDA-MB-231 cells showed a visible reduction in the fluorescence with dose-dependent treatment of **8h** due to the leakage of Rhodamine-123 from the destabilized mitochondrial membrane (Fig. 7C and 7E). In contrast, in untreated cells, mitochondria were intact with high fluorescence intensity after 48 hrs treatment. These findings collectively confirm that **8h**-induced apoptosis in MDA-MB-231 cells severely impairs cellular function.

8h-induced apoptosis is further confirmed using western blotting analysis of Bcl-2, Bax and caspase 3 protein expression in MDA-MB-231 cells. As shown in Fig. 7F, **8h** reduced the expression of Bcl-2 (anti-apoptotic protein) with the upregulation of Bax (pro-apoptotic protein), resulting in the significant Bax/Bcl-2 ratio ($P < 0.01$) compared to the control group, which is common in treated groups. The pro-and anti-apoptotic ratio of Bcl-2 subfamily members forms pores in the outer mitochondrial membrane, increasing mitochondrial membrane permeability and caspase activation, resulting in apoptosis (Warren et al. 2019). Caspase-3 expression is also increased in the **8h**-treated group. All these experimental results confirm the apoptosis-inducing potential of **8h**. Similarly, natural chalcone, xanthahumol known to exhibit apoptosis, cell differentiation and cell cycle arrest, increased ROS production, damage mitochondrial function and pro-oxidative effects at high doses (Blanquer-Rossello et al. 2013; Vesaghhamedani et al. 2022).

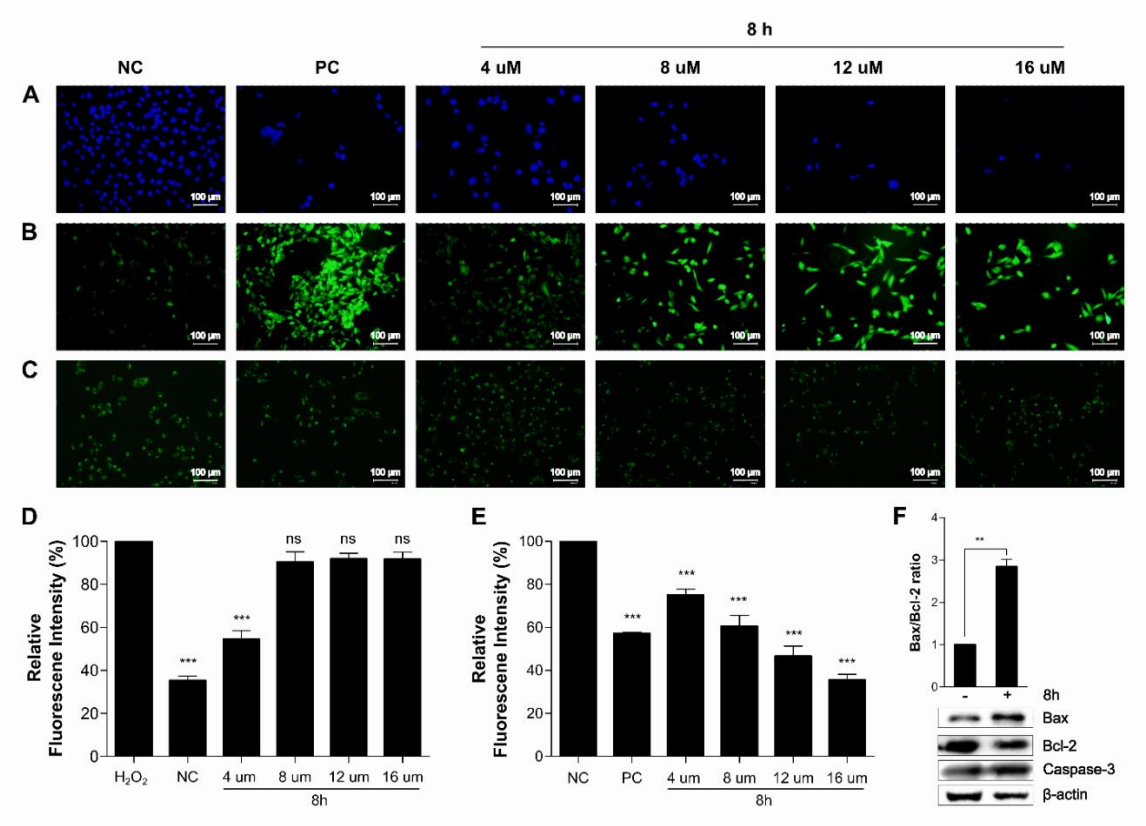

Fig. 7: Mechanistic assay to evaluate **8h** efficacy in MDA-MB-231 cells. A-C: MDA-MB-231 cells were observed under the fluorescent microscope to assess the nuclear morphological changes, ROS production and loss of MMP, resulting in cell death after 48 hrs of the treatment. A: DAPI assay, B: ROS assay, C: MMP assay. Representative images of each assay are shown. Paclitaxel (0.5 µM) and H_2O_2 are positive controls for DAPI, MMP and ROS. D-E: Fluorescence intensity was quantified using Image J software (ver. 1.54) and plotted as a Bar graph of mean±SEM (n=3) using GraphPad™ Prism 7.0 Software. F: Immunoblotting analysis of Bax, Bcl-2, and Caspase-3 expression in MDA-MB-231 cells treated with 8 µM concentrations of **8h** for 24hrs. β-actin was used as a loading control. Protein levels from each band were quantified and normalized with β-actin using Image J software (ver. 1.54). Bax/Bcl-2 ratio graphs were plotted as mean+SEM (n=3) using GraphPad™ Prism 7.0 Software applying a two-tailed paired t-test. Statistical significance was compared with respective control groups in fluorescence-based methods applying One-way ANOVA with Dunnet's multiple comparison test for fluorescence intensity. ** $P < 0.01$, *** $P < 0.001$.

3.5. Structural activity relationship

To systematically investigate the structural activity relationships (SARs) of the synthesized series of chalcone derivatives on anticancer activities, various substitutions have been done on aromatic

ring A of the chalcone, with the amide bond forming with nitrogen heterocyclic ring and amine group. SAR has been explained in the Fig. 8.

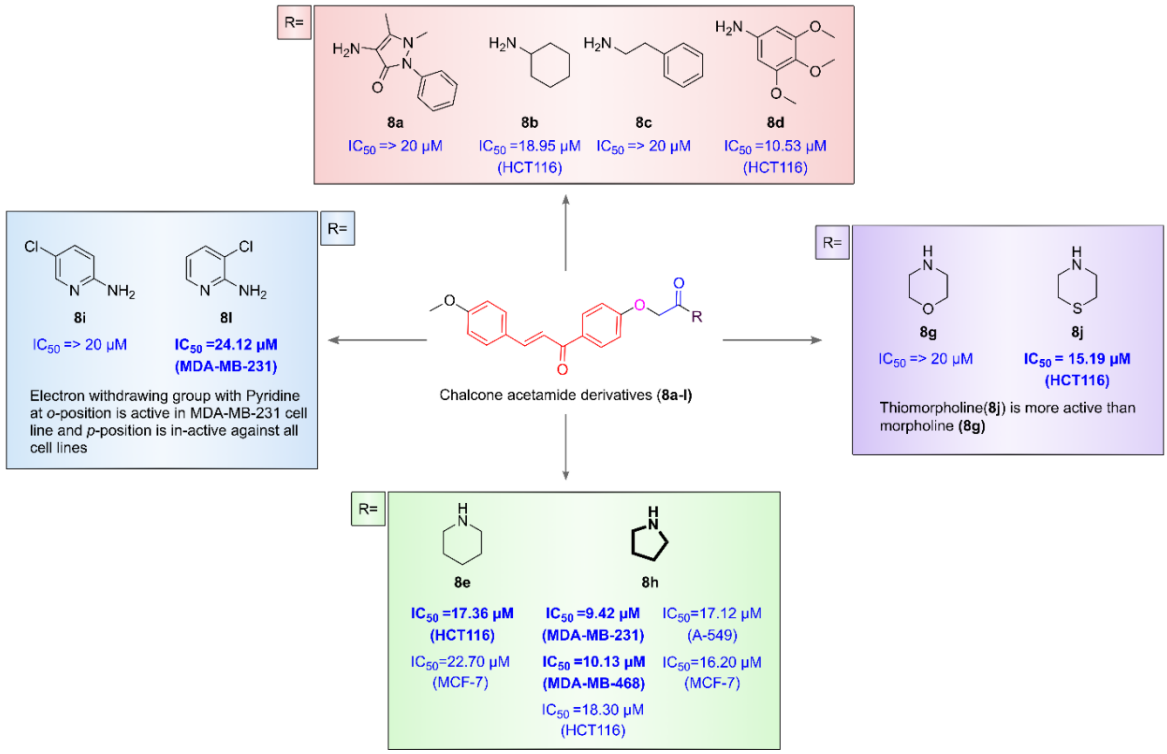

(A)- 5-membered hetrocyclic ring (Pyrrolidine-**8h**) is more favourable than 6-membered Nitrogen containg ring (Piperidine-**8e**)
(B)- Pyrrolidine(**8h**) displayed lowest cytotoxicity amomg the all derivatives on HEK-293
(4-fold less cytotoxicity in HEK293 than in MDA-MD-231 cells)
(C)- Thiomorpholine (**8j**) is more active than morpholine derivative (**8g**) against HCT-116 cell line

Fig. 8. SAR of acetamide derivatives of chalcone

4. CONCLUSIONS

In summary, a series of acetamide derivatives of chalcone were synthesized, getting a clue from the natural chalcones. Interestingly, biological results confirm that **8h** exhibited the most effective antiproliferative activity against these cell lines. The structural activity relationships (SARs) of the chalcones **8a-8l** have been postulated based on the *in vitro* cytotoxic actions. The biological activity was enhanced by including pyrrolidine ring connected to ring A with an amide bond. Since **8h** showed less toxicity than other counterparts against normal HEK293 cell line, further mechanistic studies were performed on the MDA-MB-231 cell line to prove its apoptotic mechanism behind its cytotoxicity. Additionally, **8h** caused MDA-MB-231 cells to undergo apoptosis by releasing ROS, nuclear damage and reduced mitochondrial membrane potential (MMP). Western blotting analysis demonstrated the potential ability of **8h** to induce increased apoptotic protein expression. Overall, the present research shows that chalcone derivatives with the chemical diversity of acetamide provides valuable information for designing novel compounds with enhanced safety and efficacy offering opportunities

for chemists to explore the synthesis of novel derivatives and contribute to the development of new drugs of chalcone scaffolds origin.

FUNDING STATEMENT

All authors acknowledge the support provided by the Director, CSIR-Indian Institute of Integrative Medicine, Jammu, India. PK and JSMHA are grateful for financial support through CSIR project number HCP-007. BG thanks CSIR, New Delhi, for financial support under Pan-CSIR Cancer Project (HCP-040). The institutional manuscript communication number is CSIR-IIIM/IPR/00520.

AUTHOR CONTRIBUTIONS

P.K. performed the chemical synthesis and characterization of the compounds. R.S. performed the biological activity of compounds on all cell lines. D.S performed purification of compounds. B.G. designed the biological experiments and contributed to the writing of the draft manuscript. Q.P.H. contributed to the writing of the draft manuscript. J.M.A. designed the chalcone analogs and their synthesis and contributed to the writing of the draft manuscript. All authors have approved the draft manuscript.

CONFLICT OF INTEREST STATEMENT

All authors declare there they have no conflict of interest.

DATA AVAILABILITY STATEMENT

The data that support the findings of this study are available on request from the corresponding author. The data are not publicly available due to privacy or ethical restrictions.

ORCID

Boobalan Gopu, https://orcid.org/0000-0003-2785-5650

REFERENCES

Blanquer-Rossello, M. M., J. Oliver, A. Valle, and P. Roca, 2013: Effect of xanthohumol and 8-prenylnaringenin on MCF-7 breast cancer cells oxidative stress and mitochondrial complexes expression. *J Cell Biochem*, **114,** 2785-2794.

Das, M., and K. Manna, 2016: Chalcone Scaffold in Anticancer Armamentarium: A Molecular Insight. *J Toxicol*, **2016,** 7651047.

Gao, F., M. Li, X. Yu, W. Liu, L. Zhou, and W. Li, 2021: Licochalcone A inhibits EGFR signalling and translationally suppresses survivin expression in human cancer cells. *J Cell Mol Med*, **25,** 813-826.

Gomes, M. N., and Coauthors, 2017a: Chalcone Derivatives: Promising Starting Points for Drug Design. *Molecules*, **22**.

Gomes, M. N., and Coauthors, 2017b: QSAR-driven design, synthesis and discovery of potent chalcone derivatives with antitubercular activity. *Eur J Med Chem*, **137,** 126-138.

Gottlieb, E., S. M. Armour, M. H. Harris, and C. B. Thompson, 2003: Mitochondrial membrane potential regulates matrix configuration and cytochrome c release during apoptosis. *Cell Death Differ*, **10,** 709-717.

Heer, E., A. Harper, N. Escandor, H. Sung, V. McCormack, and M. M. Fidler-Benaoudia, 2020: Global burden and trends in premenopausal and postmenopausal breast cancer: a population-based study. *Lancet Glob Health*, **8,** e1027-e1037.

Hsu, J. Y., C. J. Chang, and J. S. Cheng, 2022: Survival, treatment regimens and medical costs of women newly diagnosed with metastatic triple-negative breast cancer. *Sci Rep*, **12,** 729.

Huang, C., and Coauthors, 2020: ERalpha is a target for butein-induced growth suppression in breast cancer. *Am J Cancer Res*, **10,** 3721-3736.

Kamal, A., and Coauthors, 2010: Synthesis of imidazothiazole-chalcone derivatives as anticancer and apoptosis inducing agents. *ChemMedChem*, **5,** 1937-1947.

Khusnutdinova, E., and Coauthors, 2021: Novel A-Ring Chalcone Derivatives of Oleanolic and Ursolic Amides with Anti-Proliferative Effect Mediated through ROS-Triggered Apoptosis. *Int J Mol Sci*, **22**.

Kim, J., J. Kim, and J. S. Bae, 2016: ROS homeostasis and metabolism: a critical liaison for cancer therapy. *Exp Mol Med*, **48,** e269.

Liu, M., P. Wilairat, S. L. Croft, A. L. Tan, and M. L. Go, 2003: Structure-activity relationships of antileishmanial and antimalarial chalcones. *Bioorg Med Chem*, **11,** 2729-2738.

Marotta, L., and Coauthors, 2022: The green chemistry of chalcones: Valuable sources of privileged core structures for drug discovery. *Front Chem*, **10,** 988376.

Ouyang, Y., J. Li, X. Chen, X. Fu, S. Sun, and Q. Wu, 2021: Chalcone Derivatives: Role in Anticancer Therapy. *Biomolecules*, **11**.

Pareja, F., F. C. Geyer, C. Marchio, K. A. Burke, B. Weigelt, and J. S. Reis-Filho, 2016: Triple-negative breast cancer: the importance of molecular and histologic subtyping, and recognition of low-grade variants. *NPJ Breast Cancer*, **2,** 16036.

Rahimzadeh Oskuei, S., S. Mirzaei, M. Reza Jafari-Nik, F. Hadizadeh, F. Eisvand, F. Mosaffa, and R. Ghodsi, 2021: Design, synthesis and biological evaluation of novel imidazole-chalcone derivatives as potential anticancer agents and tubulin polymerization inhibitors. *Bioorg Chem*, **112,** 104904.

Sahu, N. K., S. S. Balbhadra, J. Choudhary, and D. V. Kohli, 2012: Exploring pharmacological significance of chalcone scaffold: a review. *Curr Med Chem*, **19,** 209-225.

Schmid, P., and Coauthors, 2020: Pembrolizumab for Early Triple-Negative Breast Cancer. *N Engl J Med*, **382,** 810-821.
Siegel, R. L., K. D. Miller, H. E. Fuchs, and A. Jemal, 2022: Cancer statistics, 2022. *CA Cancer J Clin*, **72,** 7-33.
Simirgiotis, M. J., and Coauthors, 2008: Cytotoxic chalcones and antioxidants from the fruits of a Syzygium samarangense (Wax Jambu). *Food Chem*, **107,** 813-819.
Steinlein, S., and Coauthors, 2023: Indolyl-chalcone derivatives trigger apoptosis in cisplatin-resistant mesothelioma cells through aberrant tubulin polymerization and deregulation of microtubule-associated proteins. *Front Oncol*, **13,** 1190988.
Trachootham, D., J. Alexandre, and P. Huang, 2009: Targeting cancer cells by ROS-mediated mechanisms: a radical therapeutic approach? *Nat Rev Drug Discov*, **8,** 579-591.
Trapero, A., and Coauthors, 2018: Fragment-Based Approach to Targeting Inosine-5'-monophosphate Dehydrogenase (IMPDH) from Mycobacterium tuberculosis. *J Med Chem*, **61,** 2806-2822.
Venturelli, S., M. Burkard, M. Biendl, U. M. Lauer, J. Frank, and C. Busch, 2016: Prenylated chalcones and flavonoids for the prevention and treatment of cancer. *Nutrition*, **32,** 1171-1178.
Vesaghhamedani, S., and Coauthors, 2022: Xanthohumol: An underestimated, while potent and promising chemotherapeutic agent in cancer treatment. *Prog Biophys Mol Biol*, **172,** 3-14.
Wang, Y., L. Li, T. Ma, X. Cheng, and D. Liu, 2022: Design, Synthesis, and Apoptosis-Promoting Effect Evaluation of Chalcone Derivatives Containing Aminoguanidine Units. *Anticancer Agents Med Chem*, **22,** 2116-2124.
Warren, C. F. A., M. W. Wong-Brown, and N. A. Bowden, 2019: BCL-2 family isoforms in apoptosis and cancer. *Cell Death Dis*, **10,** 177.
Yamali, C., H. I. Gul, D. O. Ozgun, H. Sakagam, N. Umemura, C. Kazaz, and M. Gul, 2017: Synthesis and Cytotoxic Activities of Difluoro-Dimethoxy Chalcones. *Anticancer Agents Med Chem*, **17,** 1426-1433.
Zhang, Z., W. Q. Chen, S. Q. Zhang, J. X. Bai, B. Liu, K. K. Yung, and J. K. Ko, 2022: Isoliquiritigenin inhibits pancreatic cancer progression through blockade of p38 MAPK-regulated autophagy. *Phytomedicine*, **106,** 154406.
Zhao, X., and Coauthors, 2017: Novel indolyl-chalcone derivatives inhibit A549 lung cancer cell growth through activating Nrf-2/HO-1 and inducing apoptosis in vitro and in vivo. *Sci Rep*, **7,** 3919.
Zhuang, C., W. Zhang, C. Sheng, W. Zhang, C. Xing, and Z. Miao, 2017: Chalcone: A Privileged Structure in Medicinal Chemistry. *Chem Rev*, **117,** 7762-7810.